Molecular Imaging and Biology (2024) 26:222–232
https://doi.org/10.1007/s11307-023-01888-5

SPECIAL TOPIC

New Horizons in Hyperpolarized ^{13}C MRI

Myriam M. Chaumeil[1,2] · James A. Bankson[3] · Kevin M. Brindle[4,5] · Shdema Epstein[6] · Ferdia A. Gallagher[7,8] · Martin Grashei[9] · Caroline Guglielmetti[1,2] · Joshua D. Kaggie[7] · Kayvan R. Keshari[10,11,12] · Stephan Knecht[6] · Christoffer Laustsen[13] · Andreas B. Schmidt[14,15,16] · Daniel Vigneron[2] · Yi-Fen Yen[17] · Franz Schilling[9,14]

Received: 20 September 2023 / Revised: 4 December 2023 / Accepted: 5 December 2023 / Published online: 26 December 2023

Abstract

Hyperpolarization techniques significantly enhance the sensitivity of magnetic resonance (MR) and thus present fascinating new directions for research and applications with *in vivo* MR imaging and spectroscopy (MRI/S). Hyperpolarized ^{13}C MRI/S, in particular, enables real-time non-invasive assessment of metabolic processes and holds great promise for a diverse range of clinical applications spanning fields like oncology, neurology, and cardiology, with a potential for improving early diagnosis of disease, patient stratification, and therapy response assessment. Despite its potential, technical challenges remain for achieving clinical translation. This paper provides an overview of the discussions that took place at the international workshop "New Horizons in Hyperpolarized ^{13}C MRI," in March 2023 at the Bavarian Academy of Sciences and Humanities, Munich, Germany. The workshop covered new developments, as well as future directions, in topics including polarization techniques (particularly focusing on parahydrogen-based methods), novel probes, considerations related to data acquisition and analysis, and emerging clinical applications in oncology and other fields.

Keywords Consensus · Hyperpolarized 13C · Metabolism · Metabolic imaging · MR spectroscopy · MRI

✉ Myriam M. Chaumeil
myriam.chaumeil@ucsf.edu

1 Department of Physical Therapy and Rehabilitation Science, University of California, San Francisco, CA, USA

2 Department of Radiology and Biomedical Imaging, University of California, San Francisco, CA, USA

3 Department of Imaging Physics, The University of Texas MD Anderson Cancer Center, Houston, TX, USA

4 Cancer Research UK Cambridge Institute, University of Cambridge, Cambridge, UK

5 Department of Biochemistry, University of Cambridge, Cambridge, UK

6 NVision Imaging Technologies GmbH, 89081 Ulm, Germany

7 Department of Radiology, Addenbrooke's Hospital, University of Cambridge, Cambridge, UK

8 Cancer Research UK Cambridge Centre, Cambridge, UK

9 Department of Nuclear Medicine, TUM School of Medicine, Klinikum Rechts Der Isar, Technical University of Munich, Munich, Germany

10 Department of Radiology, Memorial Sloan Kettering Cancer Center, New York City, NY, USA

11 Molecular Pharmacology Program, Memorial Sloan Kettering Cancer Center, New York City, NY, USA

12 Weill Cornell Graduate School, New York City, NY, USA

13 The MR Research Centre, Department of Clinical Medicine, Aarhus University, Palle Juul-Jensens Boulevard 99, Aarhus, Denmark

14 Partner Site Freiburg and German Cancer Research Center (DKFZ), German Cancer Consortium (DKTK), Im Neuenheimer Feld 280, 69120 Heidelberg, Germany

15 Division of Medical Physics, Department of Diagnostic and Interventional Radiology, Medical Center, Faculty of Medicine, University of Freiburg, Killianstr. 5a, 79106 Freiburg, Germany

16 Department of Chemistry, Integrative Biosciences (Ibio), Karmanos Cancer Institute (KCI), Wayne State University, Detroit, MI 48202, USA

17 Athinoula A. Martinos Center for Biomedical Imaging, Department of Radiology, Massachusetts General Hospital, Harvard Medical School, Boston, MA, USA

Introduction

Hyperpolarization techniques can increase the inherently low sensitivity of magnetic resonance (MR) by more than four orders of magnitude [1]. They have opened fascinating new avenues for *in vivo* MR imaging and spectroscopy (MRI/S). Hyperpolarized ^{13}C MRI/S allows real-time metabolic changes to be observed non-invasively in living organisms, including cells, tissues, animal models, and humans. In clinical research studies, hyperpolarized ^{13}C metabolic imaging has shown the potential to non-invasively improve diagnosis and monitoring of therapy in patients without the use of ionizing radiation. The only hyperpolarization technique applied in human research studies, dissolution dynamic nuclear polarization (d-DNP), was introduced 20 years ago and demonstrated the ability to detect [1-^{13}C] pyruvate metabolism in animals 15 + years ago [2], representing a breakthrough in MR metabolic imaging. However, there are many challenges for hyperpolarized ^{13}C MR to be translated to a routine clinical tool, from overcoming technical challenges (polarization, probes, and acquisition) to identifying the best clinical applications [3]. To accomplish the overwhelming promise of hyperpolarized ^{13}C MR to revolutionize medical diagnostic imaging, efforts are ongoing to improve the technique, investigate new applications, and find the best use cases for the technology. Evaluating the added clinical value of hyperpolarization techniques is currently a major challenge with more than twenty ongoing clinical trials focusing on hyperpolarized [1-^{13}C]pyruvate, the poster child of metabolic probes that employ the technique [4–6]. Novel technologies are being developed to lower the hurdle for clinical translation and allow a more widespread and reliable use of the technique. During an international workshop on "New Horizons in Hyperpolarized ^{13}C MRI" which took place on the 13th of March 2023 in the Bavarian Academy of Sciences and Humanities, Munich, Germany, recent developments ranging from hyperpolarization technology, novel probes, acquisition strategies, competing/synergistic technologies, and clinical studies were presented and discussed. In this article, we review the developments that were presented and summarize the scientific exchange that occurred during the workshop.

Latest Advances in Hyperpolarized ^{13}C MR

Technical Progress of d-DNP

The basics of d-DNP and its recent applications have been thoroughly described in a recent textbook [7]. Recent advances in this field have mostly been on the clinical side, and are discussed here and in "Clinical Studies: Scope, Acquisition, and Analysis." A major milestone in clinical application of hyperpolarized ^{13}C MRI came with the SPINlab d-DNP polarizer [8], enabling human studies at over 24 sites. This system processes up to four samples simultaneously and includes automated quality assessment steps. Recent advances in d-DNP technology include the advent of cryogen free polarizers [9, 10], polarization at high field [11], faster polarization using cross-polarization [12], and UV-light-generated radicals from the substrate itself, leading to long-lived hyperpolarized solid-state samples [13, 14]. Dedicated transport systems of such samples have been demonstrated for remote dissolution, circumventing the need for an on-site polarizer [15, 16].

The Rise of Parahydrogen-Based Methods

As an emerging option to d-DNP for preclinical and clinical hyperpolarized ^{13}C MRI, parahydrogen-based hyperpolarization methods do not require a superconducting magnet and cryogenic temperatures and were discussed with a special focus in our workshop. They potentially offer a more controllable, faster, technically less demanding, and more cost-efficient polarization procedure. Parahydrogen induced polarization (PHIP) was first predicted theoretically in 1986 by Bowers and Weitekamp and demonstrated experimentally the following year [17]. The method relies on parahydrogen as a source of the hyperpolarization, has lower equipment costs compared to d-DNP, and hyperpolarization occurs at a significantly faster rate (Fig. 1) [18–21]. However, the process typically requires organic solvents and the use of a catalyst that must be removed before exposure to the biological system. Therefore, attention has been focused on the attainment of a fully biocompatible aqueous solution of the hyperpolarized metabolite, with recent successful results, although this approach has not yet been approved for human use. Additionally, PHIP has faced limitations due to a small portfolio of agents, which includes succinate, fumarate, and a few others [22–24]. During the workshop, two main strategies based on PHIP were discussed, PHIP-SAH and SABRE, which have expanded the portfolio and are currently being extensively explored.

- Side Arm Hydrogenation (PHIP-SAH)

  This approach, pioneered by Reineri and colleagues [25], allows the application of PHIP to ^{13}C-labeled pyruvate and other biologically relevant molecules that contain a carboxylate group (Fig. 1). Feasibility has been demonstrated in metabolic studies in cells and in preclinical *in vivo* studies [26–28].

  Recently published results demonstrated that a PHIP-SAH-based [1-^{13}C]pyruvate hyperpolarization method

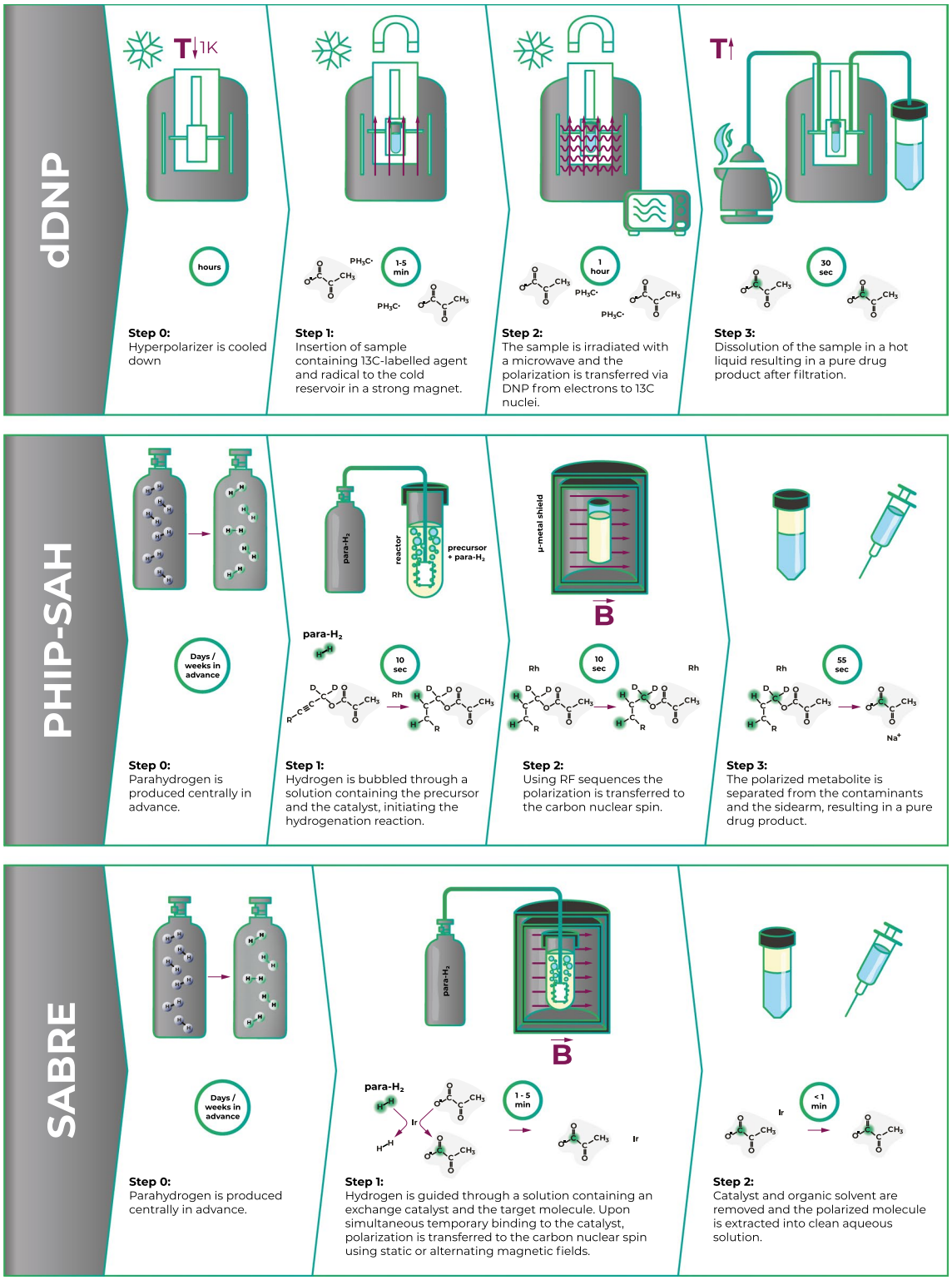

Fig. 1 Techniques comparison: d-DNP, PHIP-SAH, SABRE. Comparison between the most established ^{13}C polarization methods. d-DNP relies on transfer of polarization from free electrons under conditions of very low temperature and high magnetic field. PHIP-SAH and SABRE utilize parahydrogen as the source of polarization, transferred to the metabolite in a fast chemical reaction

with a novel purification technique achieved ~ 18% polarization at the time of injection, with comparable imaging results to d-DNP in the same animal and with an excellent safety profile over a cohort of 24 mice and 24 rats [29].

- SABRE

  Signal amplification by reversible exchange (SABRE) is a promising parahydrogen-based technique for hyperpolarizing molecules without the need for chemical modification [30] (Fig. 1). While high polarizations have been reported for many compounds [18], SABRE has recently been enabled for hyperpolarization of ^{13}C-labeled pyruvate [18, 31–33], achieving up to 22 and 6% polarization of ^{13}C at the C1 and C2 positions, respectively (prior to purification) [34]. Additionally, progress in sample purification has yielded clean aqueous pyruvate solutions with > 10% polarization, which have recently been used for the first *in vivo* metabolic MRI experiments in mice [35].

  PHIP-SAH and SABRE both have distinct advantages: SABRE does not require the synthesis of a precursor and thus is expected to be cheaper and to have fewer impurities. However, SABRE currently provides lower polarization and at lower concentrations compared to PHIP-SAH, which presents a challenge in scaling to clinical use. In addition, as the catalyst binding mechanism differs between the two methods, some probes can be more easily polarized with one method or the other. Thus, the two approaches can be considered complementary by providing together a broader range of hyperpolarized probes.

Preclinical Hyperpolarized ^{13}C MR: Current and New Applications

Most of the focus of hyperpolarized ^{13}C MR technology to date has been in the field of oncology, both for improved diagnosis and classification of tumors, as well as for monitoring therapeutic responses (see [36, 37] for recent reviews). Preclinical work in cancer is still ongoing to determine the best use cases of the technology. During the workshop, a preclinical study in estrogen receptor positive (ER +) patient-derived breast cancer xenografts treated with a phosphoinositide 3-kinase (PI3K) inhibitor was presented which demonstrated that hyperpolarized [1-^{13}C]pyruvate detected response where none could be detected using fluorodeoxyglucose-18 positron emission tomography (^{18}F-FDG-PET). The decrease in lactate labeling was shown to be a specific consequence of decreased expression of the transcription factor Forkhead box protein M1 (FOXM1) [38]. Similarly, hyperpolarized [1-^{13}C]pyruvate detected early metabolic changes in a murine model of gastric cancer in response to a pan-tyrosine kinase inhibitor when no significant changes were detected by ^{18}F-FDG-PET [39].

Beyond oncology, [1-^{13}C]pyruvate has been used recently in preclinical studies on neurological pathologies such as neurodegenerative disease and brain trauma. In a mouse model of multiple sclerosis, a new study showed hyperpolarized ^{13}C MR imaging of [1-^{13}C]pyruvate detected immunological responses to disease-modifying therapies, providing unique information on neuroinflammation and its modulation [40]. Importantly, hyperpolarized ^{13}C MRS detected response to dimethyl fumarate therapy, whereas conventional T_1 post contrast MRI did not, demonstrating the complementarity to conventional MRI. Another recent study showed that specific neuronal deletion of the glucose transporter 3 (GLUT3cKO) or pyruvate kinase 1 (PKM1cKO) in mice hippocampi led to memory impairment and metabolic changes detectable by hyperpolarized ^{13}C MRI/S [41]. Female, but not male, PKM1cKO mice had increased hyperpolarized [1-^{13}C]pyruvate-to-lactate conversion, while this ratio was decreased in female GLUT3cKO mice. ^{18}F-FDG-PET did not detect changes, highlighting the potential for hyperpolarized [1-^{13}C] pyruvate to detect downstream alterations in brain glucose metabolism. Expanding on previous work [42–44], another study explored the potential of hyperpolarized ^{13}C MR to detect long-lasting alterations in brain metabolism following repetitive mild repetitive traumatic brain injury (rTBI) in mice [45]. Decreased conversion of hyperpolarized [1-^{13}C] pyruvate to lactate, linked to decreased pyruvate dehydrogenase activity, was detected in mice after rTBI, which was not detectable with other MRI methods. Machine learning approaches showed that hyperpolarized [1-^{13}C]pyruvate can detect long-lasting metabolic impairment resulting from rTBI and predict associated behavioral changes, thereby demonstrating its potential for improving the detection and monitoring of previously undetected rTBI.

In addition to pyruvate, recent work was presented, where alternative hyperpolarized probes were used to explore other metabolic reactions *in vivo* including glutaminolysis, redox status, and fructolysis. Building on previous work [46–48], glutamine metabolism through glutaminase highlights a key way in which hyperpolarized glutamine can provide non-invasive measurement of on-target inhibition of metabolic flux [49]. As hyperpolarized pyruvate is currently used in imaging brain tumors in humans [50], using pyruvate as a solvent for other probes provide a means of overcoming previous limitations. For example, new formulations of hyperpolarized dehydroascorbate using pyruvate as a solvent potentially allow visualization of redox status in the brain [51]. Furthermore, utilizing hyperpolarized fructose [52] as an orthogonal probe of glycolysis can not only highlight differential nutrient utilization by flux through the enzyme ketohexokinase but also flux switching that occurs in cancer [53]. Ultimately, these encouraging results suggest that the field is ready to expand well beyond pyruvate as a probe *in vivo*.

Besides probing metabolism, hyperpolarized ^{13}C MR of suitable sensor molecules can be used to probe tissue properties, such as temperature, ion content, redox state, or pH. Even though pH is an important biomarker which can be crucial for disease diagnosis [54] and therapy success [55, 56], there is currently no routinely applied imaging modality in the clinic for measuring tissue pH [57]. Hyperpolarized ^{13}C MR has been successfully applied for pH imaging *in vivo* with pH sensors such as bicarbonate [58–60] and zymonic acids [61], which show an intrinsically high sensitivity to pH alterations in the physiological range. Translation of these sensors to the clinic has so far been limited by magnetization lifetime or challenging agent preparation. In contrast to hyperpolarized metabolic agents, hyperpolarized pH sensors only rely on chemical shift differences between pH-sensitive moieties. Acquisition strategies do not have to be dynamic, which enables the design of efficient acquisition techniques for improved spatial resolution. Emerging hyperpolarized pH agents, such as Z-OMPD, will likely unlock the clinical value of pH imaging, for which there is sufficient evidence in a handful of studies [62–64].

Clinical Studies: Scope, Acquisition, and Analysis

The first paper describing the production of hyperpolarized ^{13}C-labeled substrates in solution was published in 2003 [3], and the first clinical patient study with hyperpolarized [1-^{13}C]pyruvate 10 years later in 2013 [65]. The research to date has shown that hyperpolarized [1-^{13}C]pyruvate has great promise to revolutionize medical diagnostic imaging, and current studies are exploring clinical applications that have significant potential to improve patient outcome.

Most clinical applications have so far been in oncology, where it was shown, that the hyperpolarized [^{13}C] lactate signal is higher in aggressive breast, renal, and prostate cancers compared to more benign disease, with potential clinical applicability for patient stratification and for targeting biopsies [5, 66–72]. In gliomas for example, it has been demonstrated that hyperpolarized [1-^{13}C]pyruvate can detect metabolic subtypes, which can be dichotomized into more glycolytic and oxidative subtypes that have differing drug and radiation sensitivities [73, 74]. Therefore, imaging glioma patients with hyperpolarized [1-^{13}C]pyruvate could be used to help guide treatment selection. Early treatment response assessment is another promising application, where an increase in hyperpolarized [^{13}C] lactate labeling after 7–11 days of neoadjuvant chemotherapy has been demonstrated as an early response biomarker in triple-negative breast cancer [75]. Comparison of hyperpolarized imaging to tissue-based metrics of metabolism is revealing the molecular basis for these changes including the role of the pyruvate transporter (MCT1), lactate exporter (MCT4), and the enzyme lactate dehydrogenase (LDH), and can be used to explain intratumoral and intertumoral metabolic heterogeneity on imaging. In prostate cancer, elevated conversion rates of [1-^{13}C]pyruvate to [1-^{13}C]lactate (k_{PL}) have been demonstrated in more aggressive cancers, which can be utilized for improved biopsy guidance for primary organ-confined disease [72]. Another unmet clinical need that hyperpolarized ^{13}C MR can potentially address is metabolic imaging of metastatic cancers to lung and bone [76] and detection of response to therapy by assessing lymph nodes and bone metastases in prostate cancer [77]. Exciting new studies have also shown applications of [1-^{13}C]pyruvate for clinical research in renal cancer [67]. While most human studies have focused on [1-^{13}C]pyruvate, new HP probes have been translated into human studies including: [2-^{13}C]pyruvate that can detect metabolism via acetyl-CoA to acetylcarnitine, glutamate, and glutamine [78]; [1-^{13}C]alpha-ketoglutarate to detect conversion to glutamate and in mutant IDH cancers to 2-hydroxyglutarate (2-HG) [79]; and [^{13}C,$^{15}N_2$]urea that can be co-polarized with ^{13}C-pyruvate to provide unique perfusion and metabolic information simultaneously [80, 81].

Beyond oncology, applications in cardiology are also being investigated. The case for pushing hyperpolarized cardiac magnetic resonance imaging (CMR) is based on the accumulating evidence that the accuracy of conventional myocardial viability assessment is not sufficient [82]. Hyperpolarized [1-^{13}C]pyruvate CMR resembles PET/MR exams and as such could potentially replace PET/MR CMR exams in the clinical setting, if the method is either as good as FDG-PET or potentially better due to added metabolic measurements. Hyperpolarized perfusion imaging has the potential to provide as accurate perfusion information as ^{15}O-water PET, and it has been demonstrated that rest/stress pyruvate imaging is possible [83]. The current evidence suggests that hyperpolarized CMR holds great potential and that the method is ready for clinical adoption [84–89].

In renal applications, hyperpolarized [1-^{13}C]pyruvate exams have the potential to provide accurate metabolic readouts of the underlying metabolic cascades associated with kidney diseases [90]. The chronic nature and slow progression of renal disease and the low sensitivity and specificity of many biomarkers of renal dysfunction limits the ability to treat patients and develop new treatments [91, 92]. The increased sensitivity and specificity that hyperpolarized [1-^{13}C]pyruvate MRI provides could potentially be used in clinical trials as earlier markers of disease progression and thus treatment response [93–97]. As anti-fibrotic drugs are entering clinical use, methods to select patients and monitor progression will be key, and hyperpolarized [1-^{13}C]pyruvate used in combination with apparent diffusion coefficient (ADC) imaging provides the necessary sensitivity and specificity [98].

Finally, deuterium metabolic imaging (DMI) was discussed during the workshop as a new metabolic imaging technique that can potentially complement hyperpolarized ^{13}C MR. DMI was used recently to study both the metabolism of oral [6,6-$^{2}H_2$]glucose and [2,3-$^{2}H_2$]fumarate [99–101]. One of the interesting points of discussion raised during the workshop was the interplay between hyperpolarized ^{13}C MR and DMI [102], where the community was encouraged to consider what the best application for each method would be and ways in which these methods can complement each other. For example, a direct comparison between [2,3-$^{2}H_2$]fumarate and hyperpolarized [1,4-^{13}C] fumarate on the same animal has not been performed, but comparison of the results of studies [100, 103], utilizing the different agents for assessing response to treatment in the same tumor model and treatment suggests that [2,3-$^{2}H_2$] fumarate is more sensitive in detecting response to treatment, but also requires a much higher concentration and scan time and achieves a lower malate SNR. As another example, oral [6,6-$^{2}H_2$]glucose may provide complementary metrics of oxidative and reductive metabolism.

Considerations on Data Analysis

Complex, dynamic, multidimensional hyperpolarized ^{13}C MR is frequently parameterized using pharmacokinetic (PK) models or simpler area-under-the-curve (AUC) metabolite maps, or ratios of AUC maps [7]. Clinical adoption of this technology will require establishment of imaging biomarkers that are robust, reproducible, and readily interpretable. Although AUC maps and AUC ratios are straightforward to calculate, they are affected by a range of physical and physiological factors that may hinder interpretation. PK models facilitate quantification of rate constants that can reduce bias imparted by some of these factors, although care must be taken to select a PK model that balances accuracy and complexity in the context of the application [104]. The effects of confounding factors may also be minimized by careful experimental design and by acquisition of supplemental information to assess the potential impact of key sources of bias [105].

C. Hyperpolarized ^{13}C: where are we going?

The future of hyperpolarized ^{13}C technology was at the center of the scientific exchange at the workshop. Key questions that were raised included: Why is not MRI-based metabolic imaging more prevalent today, 10 years after the first publication of d-DNP use in humans? What is needed for widespread use of the technology? What important problems can the technology address? The main discussion points are summarized below and in Fig. 2.

The main point that was agreed upon unanimously was that for the technology to become scalable and impactful, the hyperpolarized ^{13}C MR technology has to be easy to use, regardless of the specific methodology and equipment employed. The following aspects were discussed:

- From the perspective of polarization, progress is being made in both d-DNP and PHIP-based polarization techniques, with methods becoming more standardized and streamlined and new polarization technologies becoming newly accessible, opening the way to larger scale preclinical and clinical studies. As such, more evidence is expected to accumulate in the coming years, paving the way towards clinical applications over a wide range of medical fields.

	Polarization	Acquisition & analysis	Application
Solved in near future	• **PHIP**-based methods with high ease of use, speed and reliability • **dDNP** more standardized	• Large existing **MRI install base** • **Image resolution and quality** comparable to PET imaging • **Acquisition and analysis schemes** standardized	• **Studies already conducted** at ~15 sites globally on ~800 healthy volunteers and patients with different diseases including cancer, heart disease, liver disease, diabetes, and more
Considerable effort still required	• **Increase polarization level** at time of injection into humans to > 50%	• MRI **X-nuclei package and coils** require extra investment	• **Multi-center** studies • **"Hero" application** - early treatment response assessment promising but larger studies needed • **Safer/cheaper alternative** to PET or Gd enhanced MRI - promising but more studies needed
	Ease of use & reliability: *Greatly improved in the near future*		**Effectiveness:** *More studies are urgently needed*

Fig. 2 The future of hyperpolarized ^{13}C: for widespread use hyperpolarized MRI needs to be easy to use, reliable, and effective. Ease of use and reliability are dependent on technological advances that are already underway and expected to become fully realized in the near future. Evidence of effectiveness requires more and larger clinical studies

- In addition to polarizers, specific MRI acquisition capabilities are required. Firstly, hyperpolarized ^{13}C MR metabolic imaging requires the MRI scanner to have ^{13}C transmit and receive capabilities. While almost all small animal MRI systems have X-nuclei capabilities (although this is not provided by the vendors as a default), it is not the case for clinical systems. Among the 35,000 clinical MRI scanners installed world-wide, only approximately 10% have X-nuclei capabilities (cf. https://stats.oecd.org/). Even more importantly, out of these only a few hundred centers are actually utilizing this capacity. This low prevalence and utilization of X-nuclei capability is likely due to the difficulties of implementing X-nuclei MRI or MRS in the clinical setting. For example, for ^{31}P MRS, 3-APP was suggested as an exogenous probe for extracellular pH [106, 107]. However, the measurement times for this pH imaging technique were long and the spatial resolution was poor, preventing wide-spread use even though it is still considered a "gold standard" for pH measurements. Furthermore, it is important to note that ~ 70% of the current MRI systems are 1.5 Tesla scanners, and to date, upgrading to X-nuclei capabilities is only available for 3 Tesla systems. This is due to vendor marketing policy and may need to change to enable wider accessibility of hyperpolarized metabolic imaging. Finally, the combined cost of adding X-nuclei capabilities (hardware and software) and radiofrequency coils might be prohibitive for most centers (> $100 K).

After "ease of use," the group unanimously took the position that robustness and reliability are a major factor required for scalability. As hyperpolarized ^{13}C MR becomes easier and more reliable, its use will increase, not only in research but also as a routine clinical tool, in a similar fashion to PET during the 1990s. Given the obvious parallel between PET and hyperpolarized ^{13}C MR, a discussion comparing the market access and potential of both methods took place. First, it was pointed out that, despite having been around for 40 years, the impact and accessibility of PET are still modest, with only ~ 5000 PET scanners worldwide, 80% of them in high income countries [108]. The lack of wider dissemination of this technology might partially be due to the need for a cyclotron, dedicated facilities with complex radiation controls, radioactive waste infrastructure and trained staff, which is a prohibitive cost for developing countries. On the other hand, the number of MRI scanners is one order of magnitude higher, with an estimate of 35,000 worldwide, with a number of about 80 million MRI exams performed per year (cf. https://stats.oecd.org/). Like PET, MRI scanners are more prevalent in high income countries, with Japan having the highest ratio of MRI units per million population (57.39 per million in 2020) followed by the USA with 38 units per million in 2021 (cf. https://stats.oecd.org/ and [109]). Finally, an issue often raised in the context of hyperpolarized ^{13}C MRI is the achievable spatial resolution, which today is around 6 mm for pyruvate and 12 mm for its products. Although this in-plane resolution is comparable to PET, the out of plane resolution of hyperpolarized ^{13}C MRI is still coarse. At the same time, there was agreement that the required resolution is driven by the individual application. As an outlook, denoising approaches are being applied broadly and could help to improve the quality of the images produced [110]. More generally, in the future, machine learning and artificial intelligence may render "image quality" (and thus resolution) less relevant if there will be a shift from relying on radiologists' interpretation that is based on images to machine-based interpretation of the raw data.

A major part of the discussion focused on potential applications of hyperpolarized ^{13}C MR, searching to find the "hero experiments" (a term which the group preferred to "killer applications"). Most participants believed that the biggest potential of this technology was for early treatment response assessment/prediction, especially in oncology. In parallel, a question was raised as to whether it is necessary for the technology to solve a current clinical unmet need to become widely useful or will it suffices to offer a safer and/or cheaper alternative to an existing tool. The recent FDA approval of hyperpolarized xenon for assessment of lung function serves as an interesting test case, as it was approved based on a non-inferiority comparison study to standard radionuclide methods rather than for a new application. One such example for a "non-inferiority" application for hyperpolarized MRI that was discussed is as an alternative contrast agent to gadolinium chelates, especially considering recent growing concerns as to the long-term safety of these agents [111]. Other potential "non-inferiority" applications are those applications for which PET is used today, e.g., in oncology, neurology, and cardiology, as discussed in "Latest Advances in Hyperpolarized 13C MR."

In conclusion, the participants shared an optimistic view about the future of hyperpolarized ^{13}C MR. Recent technological advancement on the polarization side such as the development of PHIP methods, the ongoing efforts to introduce new probes both preclinically and in first-in-man clinical studies, as well as recent community efforts towards standardization of the technology such as the International Society for Magnetic Resonance in Medicine (ISMRM) consensus group initiative and the first attempts at multicenter studies pave the way for hyperpolarized ^{13}C MR to become much easier to use and more reliable. Combined with the already widely established and available MRI infrastructure, hyperpolarized MRI has the potential to scale up quickly to more widespread usage. This will hopefully encourage larger scale preclinical and clinical studies that are urgently needed to establish the usefulness of the tool and to explore its full potential.

Funding M. M. C. is supported by grants from the National Institutes of Health (R01NS102156, R01AG064170, R01CA239462, R21AG080160, R21AI153749, and R21AI171144); the National Multiple Sclerosis Society (RG-1701-26630); the Alzheimer's Association (AARF-20-678090); and receives support from the Hyperpolarized MRI Technology Resource Center (HMTRC), funded by the National Institute of Biomedical Imaging and Bioengineering (NIH/NIBIB, P41EB013598). K. M. B. receives funding from Cancer Research UK. F. A. G. is funded by Cancer Research UK (CRUK, C19212/A27150), the CRUK Cambridge Centre, and the NIHR Cambridge Biomedical Research Centre, holds grants with GlaxoSmithKline and AstraZeneca, and receives research support from GE Healthcare. C. G. is supported by the National Institutes of Health (K99AI159380 and R21AI153749) and the National Multiple Sclerosis Society (FG-1507-05297). J. A. B is supported in part by grants from the National Institutes of Health (R01CA211150, R01CA280980, R21CA249373, and P30CA016672) and GE Healthcare. K. R. K. is supported by grants from the National Institutes of Health (R01CA237466, R01CA252037, R01CA248364, and R01CA249294) and NIH/NCICancer Center Support Grant (P30CA008748), and the Center for Molecular Imaging and Bioengineering (CMIB) at Memorial Sloan Kettering Cancer Center. C. L. is funded by the Lundbeck Foundation (R272-2017-4023 and R278-2018-620), the Danish Cancer Society (A13107, KC2018, and R279-A16251) and Karen Elise Jensen Fond (D1929347). D. V. is funded by NIH grants P41EB013598, P01CA118816, U01EB026412, R01CA256740, and R01CA238379.

Declarations

Conflict of Interest M. M. C., J. A. B., K. M. B., K. R. K., D. V., and F. S. serve on the Scientific Advisory Board of NVision Imaging Technologies. M. M. C. is a consultant for Neurona Therapeutics. S. E. and S. K. are employees of NVision Imaging Technologies. K. M. B. holds patents with GE Healthcare on some aspects of DNP technology and has a consultancy agreement with NVision Imaging Technologies GmbH. F. A. G. has consulted on behalf of the University of Cambridge for AstraZeneca. K. R. K. is co-founder of Atish Technologies, serves on the Scientific Advisory Board of Imaginostics and holds patents related to imaging and leveraging cellular metabolism. M. G., C. G., J. D. K., C. L., A. B. S. and Y. F. have no COI to disclose.

Disclaimer The content of this review is solely the responsibility of the authors and does not necessarily represent the views of its sponsors.

References

1. Witte C, Schroder L (2013) NMR of hyperpolarised probes. NMR Biomed 26(7):788–802
2. Golman K et al (2006) Metabolic imaging by hyperpolarized 13C magnetic resonance imaging for in vivo tumor diagnosis. Cancer Res 66(22):10855–10860
3. Ardenkjaer-Larsen JH et al (2003) Increase in signal-to-noise ratio of > 10,000 times in liquid-state NMR. Proc Natl Acad Sci U S A 100(18):10158–10163
4. Chaumeil MM, Najac C, Ronen SM (2015) Studies of metabolism using (13)C MRS of hyperpolarized probes. Methods Enzymol 561:1–71
5. Kurhanewicz J et al (2019) Hyperpolarized (13)C MRI: path to clinical translation in oncology. Neoplasia 21(1):1–16
6. Wang ZJ et al (2019) Hyperpolarized (13)C MRI: state of the art and future directions. Radiology 291(2):273–284
7. Larson P (ed) (2021) Hyperpolarized carbon-13 magnetic resonance imaging and spectroscopy. Elsevier Academic Press, Cambridge. https://shop.elsevier.com/books/hyperpolarized-carbon-13-magnetic-resonance-imaging-and-spectroscopy/larson/978-0-12-822269-0
8. Ardenkjaer-Larsen JH et al (2011) Dynamic nuclear polarization polarizer for sterile use intent. NMR Biomed 24(8):927–932
9. Ardenkjaer-Larsen JH et al (2019) Cryogen-free dissolution dynamic nuclear polarization polarizer operating at 3.35 T, 6.70 T, and 10.1 T. Magn Reson Med 81(3):2184–2194
10. Baudin M et al (2018) A cryogen-consumption-free system for dynamic nuclear polarization at 9.4 T. J Magn Reson 294:115–121
11. Cheng T et al (2020) A multisample 7 T dynamic nuclear polarization polarizer for preclinical hyperpolarized MR. NMR Biomed 33(5):e4264
12. Elliott SJ et al (2021) Boosting dissolution-dynamic nuclear polarization by multiple-step dipolar order mediated 1H→13C cross-polarization. J Magn Reson Open 8–9:100018
13. Eichhorn TR et al (2013) Hyperpolarization without persistent radicals for in vivo real-time metabolic imaging. Proc Natl Acad Sci U S A 110(45):18064–18069
14. Gaunt AP et al (2022) Labile photo-induced free radical in alpha-ketoglutaric acid: a universal endogenous polarizing agent for in vivo hyperpolarized (13) C magnetic resonance. Angew Chem Int Ed Engl 61(2):e202112982
15. Capozzi A et al (2021) Metabolic contrast agents produced from transported solid (13)C-glucose hyperpolarized via dynamic nuclear polarization. Commun Chem 4(1):95
16. Capozzi A (2022) Design and performance of a small bath cryostat with NMR capability for transport of hyperpolarized samples. Sci Rep 12(1):19260
17. Bowers CR, Weitekamp DP (1986) Transformation of symmetrization order to nuclear-spin magnetization by chemical reaction and nuclear magnetic resonance. Phys Rev Lett 57(21):2645–2648
18. Hovener JB et al (2018) Parahydrogen-based hyperpolarization for biomedicine. Angew Chem Int Ed Engl 57(35):11140–11162
19. Hovener JB et al (2013) A hyperpolarized equilibrium for magnetic resonance. Nat Commun 4:2946
20. Schmidt AB et al (2022) Instrumentation for hydrogenative parahydrogen-based hyperpolarization techniques. Anal Chem 94(1):479–502
21. Schmidt AB et al (2022) Quasi-continuous production of highly hyperpolarized carbon-13 contrast agents every 15 seconds within an MRI system. Commun Chem 5(1):21
22. Eills J et al (2019) Real-time nuclear magnetic resonance detection of fumarase activity using parahydrogen-hyperpolarized [1-(13)C]fumarate. J Am Chem Soc 141(51):20209–20214
23. Knecht S, Blanchard JW, Barskiy D, Cavallari E, Dagys L, Van Dyke E, Tsukanov M, Bliemel B, Münnemann K, Aime S, Reineri F, Levitt MH, Buntkowsky G, Pines A, Blümler P, Budker D, Eills J (2021) Rapid hyperpolarization and purification of the metabolite fumarate in aqueous solution. Proc Natl Acad Sci U S A 118(13):e2025383118. https://doi.org/10.1073/pnas.2025383118

24. Ripka B et al (2018) Hyperpolarized fumarate via parahydrogen. Chem Commun (Camb) 54(86):12246–12249
25. Reineri F, Boi T, Aime S (2015) ParaHydrogen induced polarization of 13C carboxylate resonance in acetate and pyruvate. Nat Commun 6:5858. https://doi.org/10.1038/ncomms6858
26. Cavallari E et al (2019) Metabolic studies of tumor cells using [1-(13) C] pyruvate hyperpolarized by means of PHIP-side arm hydrogenation. ChemPhysChem 20(2):318–325
27. Cavallari E et al (2018) The (13)C hyperpolarized pyruvate generated by ParaHydrogen detects the response of the heart to altered metabolism in real time. Sci Rep 8(1):8366
28. Hune T et al (2023) Metabolic tumor imaging with rapidly signal-enhanced 1-(13) C-pyruvate-d(3). ChemPhysChem 24(2):e202200615
29. Nagel L, Gierse M, Gottwald W, Ahmadova Z, Grashei M, Wolff P, Josten F, Karaali S, Müller CA, Lucas S, Scheuer J, Müller C, Blanchard J, Topping GJ, Wendlinger A, Setzer N, Sühnel S, Handwerker J, Vassiliou C, van Heijster FHA, Knecht S, Keim M, Schilling F, Schwartz I (2023) Parahydrogen-polarized [1-13 C]pyruvate for reliable and fast preclinical metabolic magnetic resonance imaging. Adv Sci (Weinh) 10(30):e2303441. https://doi.org/10.1002/advs.202303441
30. Adams RW et al (2009) Reversible interactions with para-hydrogen enhance NMR sensitivity by polarization transfer. Science 323(5922):1708–1711
31. Adelabu I et al (2022) Order-unity (13) C nuclear polarization of [1-(13) C]pyruvate in seconds and the interplay of water and SABRE enhancement. ChemPhysChem 23(2):e202100839
32. TomHon P et al (2022) Temperature cycling enables efficient (13) C SABRE-SHEATH hyperpolarization and imaging of [1-(13) C]-pyruvate. J Am Chem Soc 144(1):282–287
33. MacCulloch K, Browning A, Bedoya DOG, McBride SJ, Abdulmojeed MB, Dedesma C, Goodson BM, Rosen MS, Chekmenev EY, Yen YF, TomHon P, Theis T (2023) Facile hyperpolarization chemistry for molecular imaging and metabolic tracking of [1-13C]pyruvate in vivo. J Magn Reson Open 16–17:100129. https://doi.org/10.1016/j.jmro.2023.100129
34. Schmidt AB et al (2023) Over 20% carbon-13 polarization of perdeuterated pyruvate using reversible exchange with parahydrogen and spin-lock induced crossing at 50 muT. J Phys Chem Lett 14(23):5305–5309
35. de Maissin H et al (2023) In vivo metabolic imaging of [1-(13) C]pyruvate-d(3) hyperpolarized by reversible exchange with parahydrogen. Angew Chem Int Ed Engl 62(36):e202306654
36. Jorgensen SH et al (2022) Hyperpolarized MRI - an update and future perspectives. Semin Nucl Med 52(3):374–381
37. Sharma G et al (2023) Enhancing cancer diagnosis with real-time feedback: tumor metabolism through hyperpolarized 1-(13) C pyruvate MRSI. Metabolites 13(5)
38. Ros S et al (2020) Metabolic imaging detects resistance to PI3Kalpha inhibition mediated by persistent FOXM1 expression in ER(+) breast cancer. Cancer Cell 38(4):516-533 e9
39. Esfahani SA et al (2022) Hyperpolarized [1-(13)C]pyruvate magnetic resonance spectroscopic imaging for evaluation of early response to tyrosine kinase inhibition therapy in gastric cancer. Mol Imaging Biol 24(5):769–779
40. Guglielmetti C et al (2023) Imaging immunomodulatory treatment responses in a multiple sclerosis mouse model using hyperpolarized (13)C metabolic MRI. Commun Med (Lond) 3(1):71
41. Li H et al (2023) Neurons require glucose uptake and glycolysis in vivo. Cell Rep 42(4):112335
42. DeVience SJ et al (2017) Metabolic imaging of energy metabolism in traumatic brain injury using hyperpolarized [1-(13)C] pyruvate. Sci Rep 7(1):1907
43. DeVience SJ, Lu X, Proctor JL, Rangghran P, Medina JA, Melhem ER, Gullapalli RP, Fiskum G, Mayer D (2021) Enhancing metabolic imaging of energy metabolism in traumatic brain injury using hyperpolarized [1-13C]pyruvate and dichloroacetate. Metabolites 11(6):335. https://doi.org/10.3390/metabo11060335
44. Guglielmetti C, Chou A, Krukowski K, Najac C, Feng X, Riparip LK, Rosi S, Chaumeil MM (2017) In vivo metabolic imaging of traumatic brain injury. Sci Rep 7(1):17525. https://doi.org/10.1038/s41598-017-17758-4
45. Chaumeil M, Guglielmetti C, Qiao K, Tiret B, Ozen M, Krukowski K, Nolan A, Paladini MS, Lopez C, Rosi S (2023) Hyperpolarized 13C metabolic imaging detects long-lasting metabolic alterations following mild repetitive traumatic brain injury. Res Sq [Preprint]. https://doi.org/10.21203/rs.3.rs-3166656/v1
46. Cho A et al (2019) Hyperpolarized [6-(13)C, (15)N(3)]-arginine as a probe for in vivo arginase activity. ACS Chem Biol 14(4):665–673
47. Cho A et al (2018) A non-synthetic approach to extending the lifetime of hyperpolarized molecules using D(2)O solvation. J Magn Reson 295:57–62
48. Salamanca-Cardona L et al (2017) In vivo imaging of glutamine metabolism to the oncometabolite 2-hydroxyglutarate in IDH1/2 mutant tumors. Cell Metab 26(6):830-841 e3
49. Eskandari R et al (2022) Hyperpolarized [5-(13)C,4,4-(2)H(2),5-(15)N]-L-glutamine provides a means of annotating in vivo metabolic utilization of glutamine. Proc Natl Acad Sci U S A 119(19):e2120595119
50. Miloushev VZ et al (2018) Metabolic imaging of the human brain with hyperpolarized (13)C pyruvate demonstrates (13) C lactate production in brain tumor patients. Cancer Res 78(14):3755–3760
51. Patel S et al (2022) Dehydroascorbic acid: a multifaceted substrate for developing efficient DNP formulations for simultaneous assessment of multiple metabolic pathways using hyperpolarized magnetic resonance imaging. In World Molecular Imaging Congress 2022, Miami, FL, USA
52. Keshari KR et al (2009) Hyperpolarized [2-13C]-fructose: a hemiketal DNP substrate for in vivo metabolic imaging. J Am Chem Soc 131(48):17591–17596
53. Tee SS et al (2022) Ketohexokinase-mediated fructose metabolism is lost in hepatocellular carcinoma and can be leveraged for metabolic imaging. Sci Adv 8(14):eabm7985
54. Huber V et al (2017) Cancer acidity: an ultimate frontier of tumor immune escape and a novel target of immunomodulation. Semin Cancer Biol 43:74–89
55. Pilon-Thomas S et al (2016) Neutralization of tumor acidity improves antitumor responses to immunotherapy. Cancer Res 76(6):1381–1390
56. Wang BY et al (2015) Intermittent high dose proton pump inhibitor enhances the antitumor effects of chemotherapy in metastatic breast cancer. J Exp Clin Cancer Res 34(1):85
57. Anemone A et al (2019) Imaging tumor acidosis: a survey of the available techniques for mapping in vivo tumor pH. Cancer Metastasis Rev 38(1–2):25–49
58. Gallagher FA et al (2008) Magnetic resonance imaging of pH in vivo using hyperpolarized 13C-labelled bicarbonate. Nature 453(7197):940–943
59. Korenchan DE et al (2019) Using bidirectional chemical exchange for improved hyperpolarized [(13) C]bicarbonate pH imaging. Magn Reson Med 82(3):959–972
60. Bogh N et al (2020) Cardiac pH-imaging with hyperpolarized MRI. Front Cardiovasc Med 7:603674
61. Duwel S et al (2017) Imaging of pH in vivo using hyperpolarized (13)C-labelled zymonic acid. Nat Commun 8:15126

62. Granja S et al (2017) Value of pH regulators in the diagnosis, prognosis and treatment of cancer. Semin Cancer Biol 43:17–34
63. Koltai T (2020) The Ph paradigm in cancer. Eur J Clin Nutr 74(Suppl 1):14–19
64. Grashei M et al (2023) Simultaneous magnetic resonance imaging of pH, perfusion and renal filtration using hyperpolarized (13)C-labelled Z-OMPD. Nat Commun 14(1):5060
65. Nelson SJ et al (2013) Metabolic imaging of patients with prostate cancer using hyperpolarized [1-(1)(3)C]pyruvate. Sci Transl Med 5(198):198ra108
66. Ursprung S et al (2022) Hyperpolarized (13)C-pyruvate metabolism as a surrogate for tumor grade and poor outcome in renal cell carcinoma-a proof of principle study. Cancers (Basel) 14(2):335
67. Tang S et al (2021) Metabolic imaging with hyperpolarized (13) C pyruvate magnetic resonance imaging in patients with renal tumors-initial experience. Cancer 127(15):2693–2704
68. Sushentsev N et al (2022) The potential of hyperpolarised (13) C-MRI to target glycolytic tumour core in prostate cancer. Eur Radiol 32(10):7155–7162
69. Sushentsev N et al (2022) Hyperpolarised (13)C-MRI identifies the emergence of a glycolytic cell population within intermediate-risk human prostate cancer. Nat Commun 13(1):466
70. Granlund KL et al (2020) Hyperpolarized MRI of human prostate cancer reveals increased lactate with tumor grade driven by monocarboxylate transporter 1. Cell Metab 31(1):105-114 e3
71. Gallagher FA et al (2020) Imaging breast cancer using hyperpolarized carbon-13 MRI. Proc Natl Acad Sci U S A 117(4):2092–2098
72. Chen HY et al (2022) Improving multiparametric MR-transrectal ultrasound guided fusion prostate biopsies with hyperpolarized (13) C pyruvate metabolic imaging: a technical development study. Magn Reson Med 88(6):2609–2620
73. Mair R et al (2018) Metabolic imaging detects low levels of glycolytic activity that vary with levels of c-Myc expression in patient-derived xenograft models of glioblastoma. Cancer Res 78(18):5408–5418
74. Zaccagna F et al (2022) Imaging glioblastoma metabolism by using hyperpolarized [1-(13)C]pyruvate demonstrates heterogeneity in lactate labeling: a proof of principle study. Radiol Imaging Cancer 4(4):e210076
75. Woitek R et al (2021) Hyperpolarized carbon-13 MRI for early response assessment of neoadjuvant chemotherapy in breast cancer patients. Cancer Res 81(23):6004–6017
76. Chen HY et al (2020) Hyperpolarized (13)C-pyruvate MRI detects real-time metabolic flux in prostate cancer metastases to bone and liver: a clinical feasibility study. Prostate Cancer Prostatic Dis 23(2):269–276
77. de Kouchkovsky I et al (2022) Hyperpolarized 1-[(13)C]-pyruvate magnetic resonance imaging detects an early metabolic response to immune checkpoint inhibitor therapy in prostate cancer. Eur Urol 81(2):219–221
78. Chung BT et al (2019) First hyperpolarized [2-(13)C]pyruvate MR studies of human brain metabolism. J Magn Reson 309:106617
79. Kim Y et al (2023) Development of hyperpolarized [1–13C] alpha-ketoglutarate MRI for metabolic imaging of normal volunteers and mutant IDH glioma patients. In ISMRM, Toronto, ON, Canada
80. Qin H et al (2022) Clinical translation of hyperpolarized (13) C pyruvate and urea MRI for simultaneous metabolic and perfusion imaging. Magn Reson Med 87(1):138–149
81. Liu X et al (2022) Development of specialized magnetic resonance acquisition techniques for human hyperpolarized [(13) C, (15) N(2)]urea + [1-(13) C]pyruvate simultaneous perfusion and metabolic imaging. Magn Reson Med 88(3):1039–1054
82. Hunold P et al (2018) Accuracy of myocardial viability imaging by cardiac MRI and PET depending on left ventricular function. World J Cardiol 10(9):110–118
83. Joergensen SH et al (2022) Detection of increased pyruvate dehydrogenase flux in the human heart during adenosine stress test using hyperpolarized [1-(13)C]pyruvate cardiovascular magnetic resonance imaging. J Cardiovasc Magn Reson 24(1):34
84. Rider OJ et al (2020) Noninvasive in vivo assessment of cardiac metabolism in the healthy and diabetic human heart using hyperpolarized (13)C MRI. Circ Res 126(6):725–736
85. Cunningham CH et al (2016) Hyperpolarized 13C metabolic MRI of the human heart: initial experience. Circ Res 119(11):1177–1182
86. Bøgh N et al (2020) Increasing carbohydrate oxidation improves contractile reserves and prevents hypertrophy in porcine right heart failure. Sci Rep 10(1):8158
87. Bøgh N et al (2022) Initial experience on hyperpolarized [1-(13) C]pyruvate MRI multicenter reproducibility-are multicenter trials feasible? Tomography 8(2):585–595
88. Fuetterer M et al (2018) Quantitative myocardial first-pass cardiovascular magnetic resonance perfusion imaging using hyperpolarized [1-13C] pyruvate. J Cardiovasc Magn Reson 20(1):73
89. Fuetterer M et al (2022) Hyperpolarized metabolic and parametric CMR imaging of longitudinal metabolic-structural changes in experimental chronic infarction. JACC: Cardiovasc Imaging 15(12):2051–2064
90. Pedersen M et al (2020) Hyperpolarised (13)C-MRI metabolic and functional imaging: an emerging renal MR diagnostic modality. MAGMA 33(1):23–32
91. Mendichovszky I et al (2020) Technical recommendations for clinical translation of renal MRI: a consensus project of the Cooperation in Science and Technology Action PARENCHIMA. MAGMA 33(1):131–140
92. Brownlee M (2001) Biochemistry and molecular cell biology of diabetic complications. Nature 414(6865):813–820
93. Laustsen C et al (2015) Acute porcine renal metabolic effect of endogastric soft drink administration assessed with hyperpolarized [1-13c]pyruvate. Magn Reson Med 74(2):558–563
94. Laustsen C et al (2014) Insufficient insulin administration to diabetic rats increases substrate utilization and maintains lactate production in the kidney. Physiol Rep 2(12):e12233
95. Laustsen C et al (2014) High altitude may alter oxygen availability and renal metabolism in diabetics as measured by hyperpolarized [1-(13)C]pyruvate magnetic resonance imaging. Kidney Int 86(1):67–74
96. Laustsen C et al (2017) Antioxidant treatment attenuates lactate production in diabetic nephropathy. Am J Physiol Ren Physiol 312(1):F192–F199
97. Laustsen C et al (2013) Assessment of early diabetic renal changes with hyperpolarized [1-13C]pyruvate. Diabetes Metab Res Rev 29(2):125–129
98. Rasmussen CW, Bøgh N, Bech SK, Thorsen TH, Hansen ESS, Bertelsen LB, Laustsen C (2023) Fibrosis imaging with multiparametric proton and sodium MRI in pig injury models. NMR Biomed 36(2):e4838. https://doi.org/10.1002/nbm.4838
99. De Feyter HM, Behar KL, Corbin ZA, Fulbright RK, Brown PB, McIntyre S, Nixon TW, Rothman DL, de Graaf RA (2018) Deuterium metabolic imaging (DMI) for MRI-based 3D mapping of metabolism in vivo. Sci Adv 4(8):eaat7314. https://doi.org/10.1126/sciadv.aat7314
100. Hesse F, Somai V, Kreis F, Bulat F, Wright AJ, Brindle KM (2021) Monitoring tumor cell death in murine tumor models using deuterium magnetic resonance spectroscopy and spectroscopic imaging. Proc Natl Acad Sci U S A 118(12):e2014631118. https://doi.org/10.1073/pnas.2014631118
101. Hesse F et al (2022) Deuterium MRSI of tumor cell death in vivo following oral delivery of (2) H-labeled fumarate. Magn Reson Med 88(5):2014–2020
102. Kaggie JD et al (2022) Deuterium metabolic imaging and hyperpolarized (13)C-MRI of the normal human brain at

clinical field strength reveals differential cerebral metabolism. Neuroimage 257:119284
103. Gallagher FA et al (2009) Production of hyperpolarized [1,4–13C2]malate from [1,4–13C2]fumarate is a marker of cell necrosis and treatment response in tumors. Proc Natl Acad Sci U S A 106(47):19801–19806
104. Bankson JA et al (2015) Kinetic modeling and constrained reconstruction of hyperpolarized [1-13C]-pyruvate offers improved metabolic imaging of tumors. Cancer Res 75(22):4708–4717
105. Sun CY et al (2018) Influence of parameter accuracy on pharmacokinetic analysis of hyperpolarized pyruvate. Magn Reson Med 79(6):3239–3248
106. Gillies RJ, Liu Z, Bhujwalla Z (1994) 31P-MRS measurements of extracellular pH of tumors using 3-aminopropylphosphonate. Am J Physiol 267(1 Pt 1):C195-203
107. Ojugo AS et al (1999) Measurement of the extracellular pH of solid tumours in mice by magnetic resonance spectroscopy: a comparison of exogenous (19)F and (31)P probes. NMR Biomed 12(8):495–504
108. Gallach M et al (2020) Addressing global inequities in positron emission tomography-computed tomography (PET-CT) for cancer management: a statistical model to guide strategic planning. Med Sci Monit 26:e926544
109. Ogbole GI et al (2018) Survey of magnetic resonance imaging availability in West Africa. Pan Afr Med J 30:240
110. Brender JR et al (2019) Dynamic imaging of glucose and lactate metabolism by (13)C-MRS without hyperpolarization. Sci Rep 9(1):3410
111. Gulani V et al (2017) Gadolinium deposition in the brain: summary of evidence and recommendations. Lancet Neurol 16(7):564–570